Nuclear Instruments and Methods in Physics Research A 606 (2009) 806–810

Contents lists available at ScienceDirect

Nuclear Instruments and Methods in Physics Research A

journal homepage: www.elsevier.com/locate/nima

A transportable neutron radiography system based on a SbBe neutron source

J.G. Fantidis, G.E. Nicolaou *, N.F. Tsagas

Laboratory of Nuclear Technology, School of Engineering, 'Democritus' University of Thrace, Xanthi, Greece

ARTICLE INFO

Article history:
Received 25 February 2009
Received in revised form
10 April 2009
Accepted 16 April 2009
Available online 22 April 2009

Keywords:
Neutron radiography
MCNP
Thermal neutrons
SbBe source
RoHS Directive

ABSTRACT

A transportable neutron radiography system, incorporating a SbBe neutron source, has been simulated using the MCNPX code. Design provisions have allowed two radiography systems to be utilised using the same SbBe neutron source. In this respect, neutron radiographies can be carried out using the photoneutrons produced when the ^{124}Sb is surrounded by the Be target. Alternatively, γ-radiography can be utilised with the photons from the ^{124}Sb with the target removed. Appropriate collimators were simulated for each of the radiography modes. Apart from Be, the materials considered were compatible with the European Union Directive on 'Restriction of Hazardous Substances' (RoHS) 2002/95/EC, hence excluding the use of cadmium and lead. Bismuth was chosen as the material for γ-radiation shielding and the proposed system allowed a maximum activity of the ^{124}Sb up to 1.85×10^{13} Bq. The system simulated allows different object sizes to be studied with a wide range of radiography parameters.

1. Introduction

Neutron radiography (NR) is a powerful non-destructive testing technique frequently used, either on its own or as complementary to X-ray radiography, for the analysis of objects. The technique is widely used in security applications, engineering studies and industry in order to determine structural defects, geology, medicine and biological research [1,2]. Neutron radiography comprises two principal components, namely a suitable neutron beam and a device to record the image of the object studied. The necessary neutron beams used today are provided by nuclear reactors, accelerators and isotopic sources. Nuclear reactors provide high-intensity neutron beams but are expensive and non-transportable. Furthermore, a limited number of these facilities exist. Accelerator-driven neutron beams could well be used for epithermal or fast neutron imaging, but are unlikely to generate sufficiently high neutron fluxes for thermal neutron imaging. The necessary accelerators lack transportability and are expensive. Isotopic neutron sources, although of low neutron intensity in comparison to accelerators and nuclear reactors, may be incorporated in transportable units, offering the possibility for in-situ testing of objects. Furthermore, their low cost implies that they can be acquired by more laboratories.

In this work, a transportable unit for radiography, based on the use of thermal neutrons from an SbBe isotopic neutron source incorporated within it, has been simulated using the MCNPX Monte Carlo code [3]. The aim is to optimize the design of the unit in terms of the envisaged moderator, collimator and shielding, rendering it suitable for in-situ quality non-destructive testing, while ensuring adequate radiation protection measures for the personnel in the neighborhood of the unit. The proposed unit is designed according to article 4 of the RoHS Directive 2002/95/EC, regarding the choice of materials. Hence, lead, mercury, cadmium, hexavalent chromium, polybrominated biphenyls (PBB) and polybrominated diphenyl ethers (PBDE) have been excluded [4]. An exception has been made for beryllium (Be), which is necessary as target in the SbBe source.

2. Materials and methods

2.1. The neutron source

The SbBe neutron source effectively comprises two parts: the ^{124}Sb isotope and a Be target. Neutrons are formed from the interaction of the photons emitted from ^{124}Sb ($\tau_{1/2}=60.2$ days, $E_\gamma=1.691$ MeV) with the Be through the photoneutron reaction ^{9}Be (γ, n) ^{8}Be. The γ-ray spectrum from the decay of ^{124}Sb, which was experimentally derived by Patil et al. [5], has been used for the purposes of this paper. The threshold energy of the reaction is about 1.667 MeV.

The source emits neutrons with a 'soft' spectrum having a mean energy at 24 keV and a small fraction of fast neutrons. Bücherl et al. [6,7] have simulated, using the MCNPX code, the neutron spectrum with an excellent agreement to experimental results. The probability of photoneutron production by one photon of energy E is given by the following equation:

$$w(E)=\frac{\sigma_{(\gamma n)}(E)}{\sigma_{tot}(E)}(1-\exp[-\sigma_{tot}(E)n\Delta]) \quad (1)$$

* Corresponding author.
E-mail address: nicolaou@ee.duth.gr (G.E. Nicolaou).

0168-9002/$ - see front matter © 2009 Elsevier B.V. All rights reserved.
doi:10.1016/j.nima.2009.04.016

where $w(E)$ is the neutron yield per photon emitted by the ^{124}Sb, $\sigma_{\gamma n}$ the photoneutron reaction cross-section, σ_{tot} the total photon scattering and absorption cross-section, and n and Δ are the density and thickness of the Be target [8]. According to Eq. (1), the neutron yield is proportional to the thickness of the Be target. However, an increase in thickness would be accompanied by an increase in the overall dimensions and weight of the unit. Hence, the choice of the Be target is a compromise between beam intensity and transportability for in-situ testing.

The source has effectively an on/off switching capability since the removal of the Be target would terminate the production of the neutrons. This renders the transportation of the source easier since only shielding for the photons emitted by ^{124}Sb would be required. The emitted high-energy photons could be used, with the Be target removed, for γ-radiography of volumetric dense objects. The source emits a large number of photons with energy higher than common isotopic sources like ^{137}Cs and ^{60}Co, which are widely used in industrial applications. Hence, the plurality of the photons with energy of 1.691 MeV from the ^{124}Sb source could be suitable for γ-radiography for bulky dense objects. The source has two main disadvantages: the short half-life of 60.2 days and the high specific γ-activity of ^{124}Sb. The first can be overcome by an appropriate design allowing more than one objects being simultaneously analysed by neutron or γ-radiography. The second can be surpassed using gamma-insensitive neutron detection plates [9,10] and with image filtering in digital radiography [7].

2.2. Simulation of the radiography unit

The radiography unit is designed in the form of a sphere with a radius of 42.5 cm, which rests on an Iron (Fe) base. Side and cross-sectional views through the centre of the unit are shown in Fig. 1. The SbBe source is symmetrically placed at the centre of the sphere (POS 2). The ^{124}Sb part of the source has been simulated as a vertical cylinder with 0.42 cm radius and 6 cm height. It is surrounded by the Be target of 2.58 cm thickness and 6 cm height. According to Eq. (1), an ^{124}Sb source with an activity of 1.85×10^{13} Bq is considered yielding 2×10^{9} n/s.

The photoneutrons produced, with an average energy of about 24 keV, are moderated down to thermal energies using polyethylene (PE). Hence, a 1-cm-thick PE surrounds the Be target providing the necessary thermalisation of the photoneutrons and a maximum thermal neutron flux at the collimator inlet aperture. The sphere is made of bismuth (Bi), which provides the necessary shielding against the photons from the source. A layer of borated polyethylene (PE–B) with 1 cm thickness surrounds the sphere in order to eliminate any thermal neutrons diffusing out of the unit. The design offers the possibility to lower down to POS 1 the Be target and the PE that surrounds it, hence stopping the production of neutrons. This would allow the direct use of the ^{124}Sb photons for γ-radiography with the appropriate collimator.

During the use of the unit, the conic-shaped shielding sectors S1 and S2 can be removed to allow placing collimators in order to provide a path for the neutrons from the source towards the objects being imaged (Fig. 1). Fig. 2 shows the unit with a neutron and a γ-collimator in positions S2 and S1, respectively. The collimator being used for NR comprises two parts. The first, attached to the PE moderator, which is around the Be target, is a PE tube with a wall thickness of 3 cm, inner radius of 3 cm and length of 11 cm. The space within the tube can be filled with a crystal Bi block to filter the photons from the ^{124}Sb emitted towards the object. Crystal Bi is commonly used for photon filtration, since it provides similar photon attenuation with lead, while not attenuating the neutron beam. Next to the PE tube is a divergent collimator determining to a great extent the quality of the image for a given source type. The material used in the design of the collimator should prevent stray and scattered neutrons from reaching the object through absorbing them, hence improving the unsharpness of the image obtained. In this respect, the lining of the collimator, towards reducing the scattering of neutrons within it, is particularly important and it should be made of a neutron-absorbing material [11]. The collimator inner lining is composed of a 0.8 cm layer of boral. The external surface of the collimator is made of a 3 cm layer of PE–B, there is a 1 cm layer of Bi sandwiched between the two materials, preventing stray photons from arriving at the object.

The collimator ratio (L/D) determines the quality of the NR imaging for a given design of the collimator, which is governed by the equations

$$\phi_\iota = \frac{\phi_\alpha}{16(L_S/D)^2} \tag{2}$$

and

$$u_g = L_f\frac{D}{L_s} \tag{3}$$

where L_f is the image surface to object distance, L_s is the source to object distance, D is the inlet aperture diameter, φ_i is the neutron flux at the image plane, φ_α is the neutron flux at the aperture, and u_g is the geometric unsharpness.

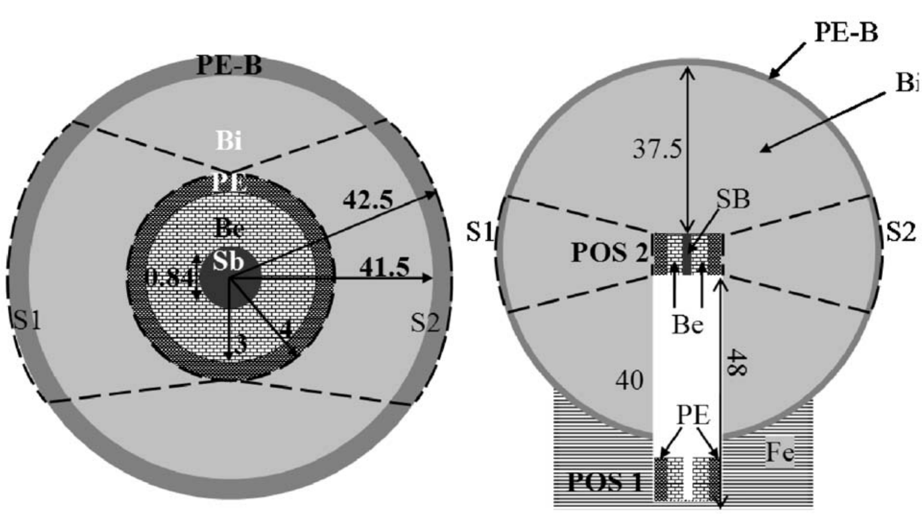

Fig. 1. Top and side view of the mobile SbBe source—not in scale (all dimensions in cm).

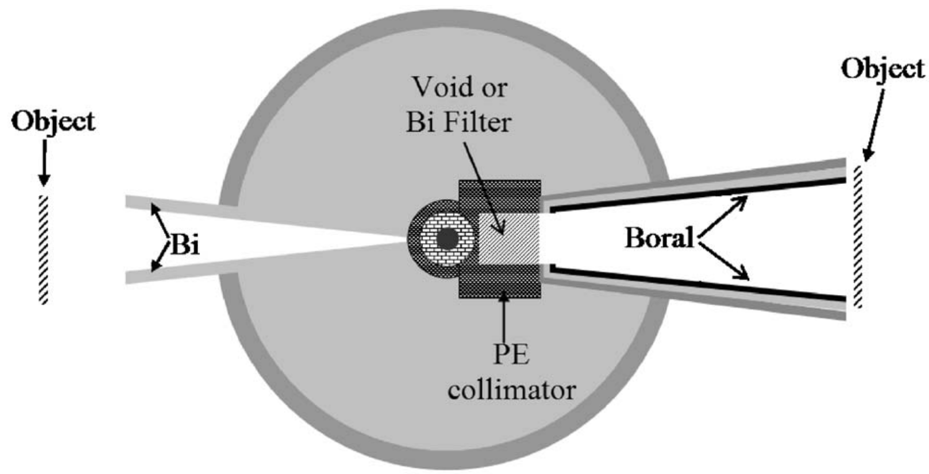

Fig. 2. Geometric configuration of the suggestion layout with the two different types of collimators—not in scale.

In addition, the beam divergence is a significant measure of the effectiveness of the beam next to its periphery. If the neutron beam diverges very rapidly, then the outer parts of the images produced could be significantly distorted. The half-angle of the beam divergence (θ) is given by [11]

$$\theta = \tan^{-1}\left(\frac{I}{2L}\right) \tag{4}$$

where I and L are the maximum dimension of the image plane and the length of the collimator, respectively. The imaging quality of a system would be further characterized by the Thermal Neutron Content (*TNC*), which describes the number of thermal neutrons within the neutron beam

$$TNC = \frac{\textit{thermal neutron flux}}{\textit{total neutron flux}} \tag{5}$$

and the relative intensities of the neutron (n) and the photon (γ) components of the beam (n/γ). Hawkesworth [12] has shown that the least recommended value is about 500 $\mathrm{cm^{-2}\,mSv^{-1}}$. However, since digital radiography would allow fast image-processing (spatial, average, median and sharpening filters) with better results [6] and the development of new gamma-insensitive neutron detection plates, a ratio less than this can also be justified.

The use of the ^{124}Sb source for γ-radiography requires a dedicated collimator, which is shown in position S1. A divergent collimator made of 8-cm-thick Bi walls was used. The first 37.5 cm of the collimator wall was provided by the Bi spherical unit itself while the total length could be extended according to the application. In the case of γ-radiography, the geometric unsharpness for different significant object thicknesses is given by

$$U_g = f\frac{b}{a} \tag{6}$$

where f is the source focal-spot size, a is the distance from the source to front surface of the object, and b is the thickness of the object.

Codes and standards used in industrial radiography require that the geometric unsharpness is as small as possible. In general, the allowable amount is 1/100 of the material thickness up to a maximum of 0.1 cm [13].

3. Results and discussion

The system was designed under the constraint that the Dose Equivalent Rate (*DER*) would remain below the annual occupational dose limit of 0.5 Sv (or 25 μSv $\mathrm{h^{-1}}$) at a distance of 50 cm from the surface of the unit. The total dose rate, due to the neutrons and photons, was calculated with the MCNPX Monte Carlo code, using the F4, Fm4 tallies and the DE, DF cards. The F tallies describe the neutron flux within a cell, while the D cards convert the absorbed dose to equivalent dose. Calculations were performed for a total number of histories per starting particle (*NPS*) of 3×10^6, yielding an accuracy in the calculations of $<1\%$. The resulting total *DER* is 16.5 μSv $\mathrm{h^{-1}}$ at 50 cm away from the unit surface, with the ^{124}Sb source and Be target in position 2. The total dose, which is below the occupational dose limit, comprises the neutron and photon components with values of 15.2 and 1.3 μSv $\mathrm{h^{-1}}$, respectively. The induced photons from the interaction of the neutrons and the PE moderator material result in a dose that is about three orders of magnitude less than the dose from the ^{124}Sb photons. Hence, the dimensions of the proposed unit, satisfying the occupational dose limit, constraint are approximately $85\times85\times93$ cm ($W\times L\times H$) and the overall weight is about 2150 kg.

The proposed NR collimator has been considered with a variable collimator length ($L = 120$–600 cm), variable diameter of its aperture next to the image plane ($D_0 = 12$–60 cm), a divergence angle (θ) of the beam of 2.85° and an inlet aperture (D) of the collimator of 6 cm. The distance (L_f) between the object and the imaging detector was considered at 0.5 cm [11]. Calculations were carried out in order to determine the PE collimator length, which would give the maximum thermal neutron flux at the object. The length was determined to be 11 cm. The variation of the thermal neutron flux at the field of view at the object position was within 1.6%.

The thermal neutron flux (f_{th}), *TNC* and (n/γ) parameters calculated are shown in Table 1 for different collimator parameters, with and without the crystal Bismuth filter. The neutron flux was calculated with the aid of the MCNPX code using the F2 tally, which gives the required neutron and photon flux averaged over a surface in neutrons $\mathrm{cm^{-2}}$ per starting neutron. Calculations were carried out with $NPS = 5\times10^6$ and 5×10^8 histories for neutrons and photons yielding an accuracy $<1\%$. An energy boundary of 0.01–0.3 eV was used to score the thermal neutron flux. According to Table 1 the *TNC* and the (n/γ) parameters remain approximately stable for the different collimator parameters.

The f_{th}, *TNC* and (n/γ) parameters were determined for different Bi filter thicknesses in the case of three L/D values (Table 2). The thermal neutron flux varies from 3.8×10^3 up to 9.6×10^1 $\mathrm{n\,cm^{-2}\,s^{-1}}$ for a maximum activity of the ^{124}Sb equal to

Table 1
The NR calculated parameters using the proposal system.

				NR calculated parameters without crystal Bismuth filter			NR calculated parameters with 11 cm crystal Bismuth filter		
L (cm)	L/D (cm)	D_0 (cm)	U_g (cm)	f_{th}	TNC (%)	n/γ (cm^{-2}Sv^{-1})	f_{th}	TNC (%)	n/γ (cm^{-2}Sv^{-1})
120	20	12	2.50E−2	3.79E+3	21.9	51.5	2.37E+3	65.2	958
180	30	18	1.67E−2	1.91E+3	21.8	51.2	1.07E+3	65.0	956
240	40	24	1.25E−2	9.47E+2	21.4	51.2	5.93E+2	65.2	950
300	50	30	1.00E−2	6.13E+2	21.2	51.0	3.91E+2	65.2	955
360	60	36	8.33E−3	4.25E+2	21.2	50.7	2.67E+2	65.2	949
420	70	42	7.14E−3	3.23E+2	21.6	50.4	1.97E+2	65.3	960
480	80	48	6.25E−3	2.43E+2	21.4	50.6	1.53E+2	65.3	948
540	90	54	5.56E−3	1.95E+2	21.3	50.7	1.19E+2	65.2	954
600	100	60	5.00E−3	1.56E+2	21.2	50.3	9.55E+1	65.6	956

Table 2
The NR calculated parameters for three L/D values with variable crystal Bismuth filter length.

	$L/D=20$			$L/D=50$			$L/D=100$		
Bi filter (cm)	f_{th}	TNC (%)	n/γ (cm^{-2}Sv^{-1})	f_{th}	TNC (%)	n/γ (cm^{-2}Sv^{-1})	f_{th}	TNC (%)	n/γ (cm^{-2}Sv^{-1})
0	3.79E+3	21.9	51.5	6.13E+2	21.2	52.4	1.56E+2	21.2	50.3
1	3.71E+3	24.3	87.7	6.05E+2	24.4	88.2	1.54E+2	24.3	86.7
2	3.61E+3	28.1	129	5.95E+2	27.5	134	1.51E+2	27.4	127
3	3.53E+3	32.3	183	5.83E+2	32.1	185	1.48E+2	31.9	181
4	3.43E+3	35.8	237	5.69E+2	35.6	239	1.43E+2	35.6	240
5	3.33E+3	39.7	323	5.51E+2	39.9	315	1.38E+2	39.9	316
6	3.19E+3	44.2	414	5.27E+2	44.2	404	1.32E+2	44.0	407
7	3.05E+3	49.4	557	5.03E+2	49.4	545	1.25E+2	49.3	551
8	2.87E+3	54.0	656	4.81E+2	53.8	669	1.19E+2	53.6	661
9	2.71E+3	58.4	769	4.51E+2	58.4	770	1.11E+2	58.1	765
10	2.53E+3	61.2	851	4.19E+2	61.3	849	1.04E+2	61.3	862
11	2.37E+3	65.2	957	3.91E+2	65.4	952	9.55E+1	65.6	956

1.85×10^{13} Bq, the TNC varies from 21–65% and the (n/γ) range from 50 up to 950 mSv h^{-1}. Good-quality thermal neutron images require exposures of the order of 10^7 n cm^{-2} [14,15], with the exposure time being proportional to the thermal neutron flux. In the case of $L/D=20$, the exposure time varies between 44 and 70 min without filter and with the 11 cm crystal bismuth filter, respectively. Higher L/D values would require higher exposure time: in the cases of $L/D=50$ and 100, exposure times in the range 4.48–7.13 and 18.5–30.2 h would be required, respectively.

The proposed system was further simulated, with the MCNPX code, for γ-radiography, making use of the fact that the ^{124}Sb is a strong photon emitter. Photon fluxes were calculated using the F2 tally with $NPS=10^8$ histories yielding an accuracy $<0.5\%$ (Table 3). The system has been considered with a variable collimator length ($L=40$–120 cm), variable source-to-object distance ($a=100$–300 cm) and divergence angle ($\theta=3.43°$–$5.71°$). In order to determine the u_g, the thickness of the object was assumed to be 20 cm. A source focal-spot size (f) of 0.5 cm was considered in order to keep u_g below the recommended value of 0.1 cm. The collimation system has been designed to obtain a spot of 12–60 cm in diameter of the photon beam at the object position.

Table 3
The calculated parameters for X-ray radiography system, with 20 cm thickness of the object and 0.5 cm source focal-spot size (all values for 1.691 MeV photons).

L (cm)	a (cm)	Spot size (cm)	θ (°)	u_g (cm)	F_γ* (1.691 MeV)	Uncollided γ (%)
40	100	12	3.43	1.00E−1	4.05E−8	97.1
50	120	18	4.29	8.33E−2	3.23E−8	96.8
60	150	24	4.57	6.67E−2	2.17E−8	97.0
70	170	30	5.04	5.88E−2	1.84E−8	97.1
80	200	36	5.14	5.00E−2	1.37E−8	96.9
90	220	42	5.45	4.55E−2	1.25E−8	97.3
100	240	48	5.71	4.17E−2	1.05E−8	96.3
110	270	54	5.71	3.70E−2	8.59E−9	96.3
120	300	60	5.71	3.33E−2	6.71E−9	96.4

p cm^{-2} s^{-1} per starting photon.

4. Conclusions

A transportable system using an SbBe source has been simulated, for radiography purposes, using the MCNPX Monte Carlo code. Except for Be, all the other materials considered were chosen according to the EU Directive 2002/95/EC, hence excluding lead and cadmium. Hence, Bi was used to shield the photons emitted by the source, reducing the dose to its surrounding to below the occupational dose limits. The fact that the presence of the Be around the ^{124}Sb leads to the neutron production has led to a design that foresees the removal of the Be target. Hence, further to the NR, the option for γ-radiography using directly the photons from ^{124}Sb can be materialised using the photoneutrons. Appropriate collimators have been simulated for the two radiography options. The use of crystal Bi within the collimator for NR has led to improved parameters associated with NR. According to the results obtained, the proposed system has a wide range of values for the parameters characterising the neutron and γ-radiographies, resulting in radiographs of variable quality.

References

[1] C.O. Fischer, J. Stade, W. Bock, in: Proceedings of the fifth World Conference on Neutron Radiography, Berlin, Germany, June 17–20, 1996.
[2] W.J. Lewis, L.G.I. Bennett, T.R. Chalovick, O. Francescone, in: 15th World Conference on Nondestructive Testing, Roma, Italy, October 15–21, 2000.
[3] D.B. Pelowitz, MCNPXTM User's Manual Version 2.5.0, 2005.
[4] B. D'Mellow, D.J. Thomas, M.J. Joyce, P. Kolkowski, N.J. Roberts, S.D. Monk, Nucl. Instr. and Meth. A 577 (2007) 690.
[5] Amol Patil, D. Santhosh, K. Vijay Sai, M. Sainath, K. Venkataramaniah, Appl. Radiat. Isot. 64 (2006) 693.
[6] T. Bücherl, N. Kardjilov, C.L. von Gostomski, E. Calzada, A.M. El Ghobary, Appl. Radiat. Isot. 61 (2004) 659.
[7] T. Bücherl, N. Kardjilov, Ch. Lierse von Gostomski, E. Calzada, IEEE Trans. Nucl. Sci. NS52 (2005) 342.
[8] D.A. Gryaznykh, V.A. Lykov, V.V. Plokhoi, Nucl. Instr. and Meth. 448 (2000) 106.
[9] S. Masalovicha, A. Ioffea, M. Schlappa, H. von Seggernb, E. Küssel, Th. Brückel, Nucl. Instr. and Meth. 539 (2005) 236.
[10] G.A. Appleby, C.M. Bartle, G.V.M. Williams, A. Edgar, Curr. Appl. Phys. 6 (2006) 389.
[11] J.C. Domanus, Collimators for Thermal Neutron Radiography—An Overview, D. Reidel Publishing Company, 1987.
[12] M.R. Hawkesworth, At. Energy Rev. 15 (2) (1977) 169.
[13] R.A. Quinn, C.C. Sigl, Radiography in Modern Industry, fourth edition, Rochester, New York Eastman Kodak Company, 2001.
[14] K. Gibbs, H. Berger, T. Jones, D. Polansky, J. Haskins, D. Schneberk, J. Brenizer, in: ASNT Fall Conference, October 1999.
[15] http://www.ati.ac.at.